

## Supplementary Information for

Hg compound-specific isotope analysis (CSIA) at ultra-trace levels using an on line gas chromatographic pre-concentration and separation strategy coupled to multicollector-ICP-MS

Sylvain Bouchet<sup>†</sup>, Sylvain Bérail and David Amouroux

CNRS / Univ Pau & Pays Adour, Institut des sciences analytiques et de physico-chimie pour l'environnement et les matériaux, UMR5254, 64000, Pau, France

*<sup>†</sup>Present address: ETH Zürich, D-USYS department, Universitätstrasse 16, CH-8092 Zürich, Switzerland*

\*Corresponding author: [sylvain.bouchet@usys.ethz.ch](mailto:sylvain.bouchet@usys.ethz.ch); +41 58 765 5461

## Table of contents

Figure SI-1. Schematic representation of the hyphenation between the PTV-GC and the MC-ICP-MS instrument.....	3
Figure SI-2. Screenshot from the GC software showing the time-course of the inlet temperature and gas flow during the different PTV program steps.....	4
Figure SI-3. Signal intensities of Hg species and duration of the plasma perturbation as a function of the PTV parameters; Peak areas of Hg species as a function of the injected volume.....	5
Figure SI-4. Calibration curves obtained for low level Hg species concentration.....	6
Table SI-1. Hg species concentrations measured in the various environmental RMs by regular GC/Q-ICP-MS and PTV-GC/Q-ICP-MS.....	7
Figure SI-5. Typical example of a GC/MC-ICP-MS chromatogram displaying the Hg and TI signals and isotopic ratios .....	8
Figure SI-6. Typical examples of GC/Q-ICP-MS chromatograms obtained for the various injection volumes.....	9
Figure SI-7. Internal precision on the $^{202/198}\text{Hg}$ isotopic ratio measurements for the NIST SRM-3133 IHg standard and STREM MMHg standard as a function of the Hg mass injected and peak areas.....	10
Figure SI-8. Isotopic compositions of IHg NIST SRM-8610 and MMHg STREM standards versus NIST SRM-3133 as a function of the injected volume. ....	11
Table SI-2. Injected volumes and the corresponding Hg concentrations in the organic solvent (hexane).....	11
Figure SI-9. Distribution of the complementary MIF values (with respect to Figure 3) over 2 years of the NIST SRM-8610 and STREM standards.....	12
Figure SI-10. Example of $\delta^{202}\text{Hg}$ STREM values calculated by CUB and CSB and confronted to the peak area sensitivity ratio between the STREM and NIST 3133 standards.....	13
Figure SI-11. Typical chromatogram obtained for the NRC TORT-2.....	14

## Supplemental Methods

For GC/Q-ICP-MS, working solutions of TI were prepared from a  $1000\ \mu\text{g}\cdot\text{mL}^{-1}$  stock solution (Spex Certiprep, USA) by dilution in 1%  $\text{HNO}_3$  while working solutions for Hg species were diluted in 1%  $\text{HCl}$  from stock solutions of IHg ( $6300\ \mu\text{g}\cdot\text{mL}^{-1}$ , made from a Hg chloride salt, Sigma Aldrich) and MMHg ( $7200\ \mu\text{g}\cdot\text{mL}^{-1}$ , made from a MMHg chloride salt, Strem chemicals Inc., Bischheim, France).

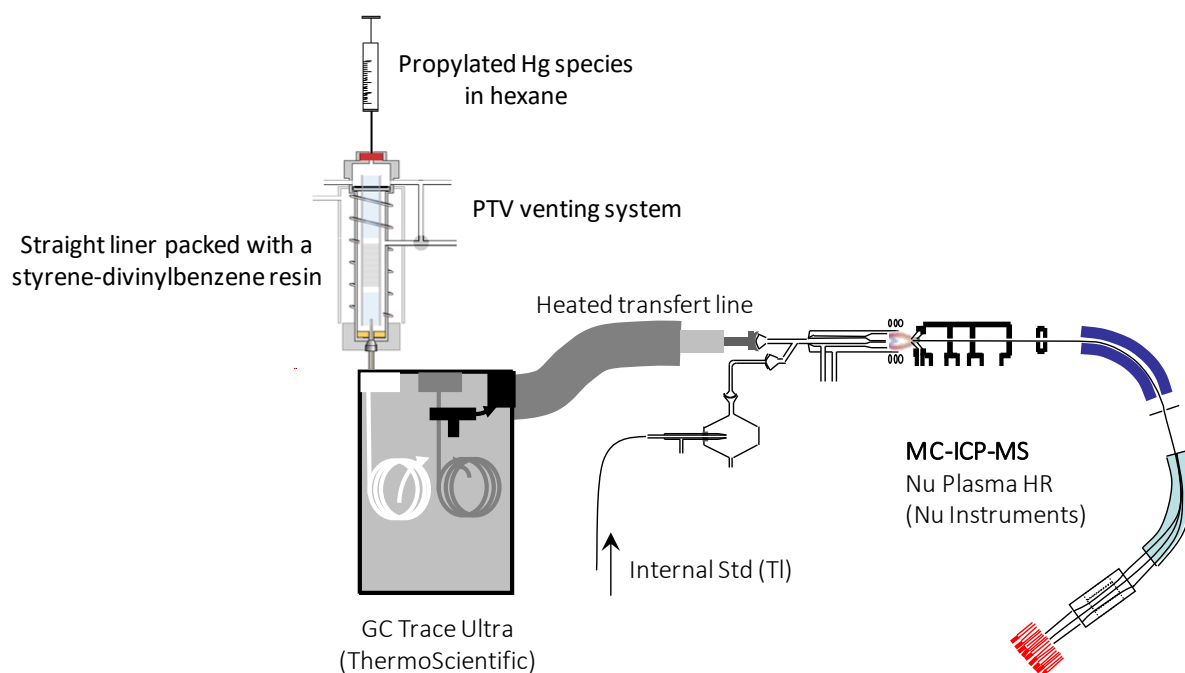


**Figure SI-1.** Schematic representation of the hyphenation between the PTV-GC and the MC-ICP-MS instrument. The PTV part is actually built in an injection port of the GC but it is here enlarged and offset from the GC for the sake of clarity.

Preliminary experiments were carried out with GC/Q-ICPMS to investigate the basic parameters of the PTV program (data not shown). The desorption and transfer of Hg species from the liner to the column head was found to be complete with a transfer step at  $200\ ^\circ\text{C}$  lasting 1 min; below that temperature, some IHg remained in the liner. The ramping rate from the initial to the transfer temperature was set at the maximum value ( $10\ ^\circ\text{C}\cdot\text{s}^{-1}$ ) allowed by the instrument given that no degradation of Hg species were observed under such conditions. After the transfer step, a cleaning phase was added at  $225\ ^\circ\text{C}$  for 2 min and under a higher He flow ( $75\ \text{mL}\cdot\text{min}^{-1}$ ) to remove less volatile compounds that may have also adsorbed. A chart of the temperature and gas flow rate during the various PTV steps is given below in Figure SI-2. Various amounts of sorbent were tested between 20 and 30 mg and the optimum was found to be within 25-27 mg (ca 3.5 cm height in the liner) when considering both the efficiency of species retention but also the peak shapes. Below this amount, the maximum volume(s) injectable 'at-once' or by multiple injections was limited while above the peaks became too wide, distorted or even doubled (data not shown).

*Venting parameters.* The basic parameters of the PTV program are shown in Figure SI-2. Figure SI-3 a, b and c presents the variations in signal intensities for each Hg species and the duration of the plasma perturbation by the solvent elution (assessed by the duration length of the drop in the TI signal) according to the inlet temperature, venting gas flow and duration, respectively. Regarding the inlet temperature, the signal intensities of Hg species are highest between 35 and 40 °C and reduced thereafter with losses at 60 °C reaching 12-13 % while the duration of the plasma perturbation decreases from 50 to 35 s between 35 and 60 °C. The plasma perturbation drops more than twice, from 98 to 43 s, when the venting time increases from 0.1 to 0.5 min and then remains stable. On the other hand, the Hg species signals markedly increase (70 %) from 0.1 to 0.3 min and then remain constant. Similarly, the plasma perturbation declines from 79 to 35 s when the venting flow is turned up from 50 to 150 mL.min<sup>-1</sup> whereas no significant changes are observed for Hg species over that range. Considering both signal responses, those three parameters were set as follow: inlet temperature 40 °C, venting time 0.5 min and venting flow 100 mL.min<sup>-1</sup>.

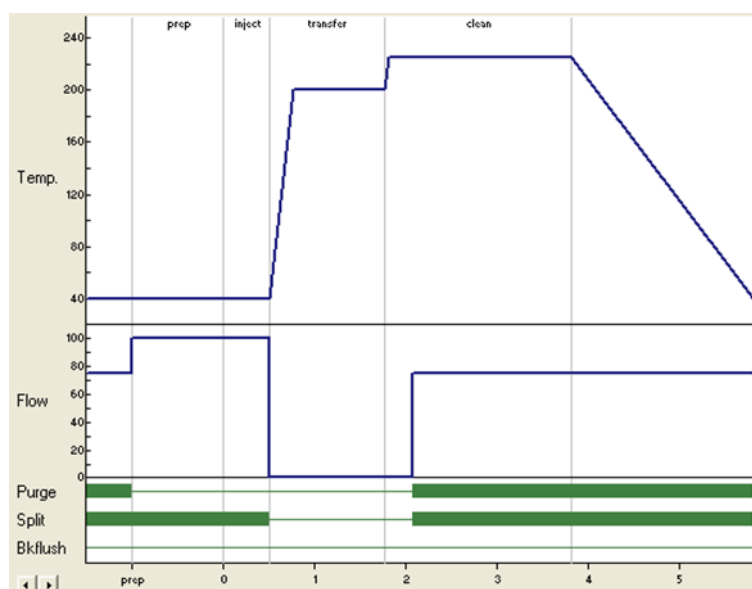


**Figure SI-2.** Screenshot from the GC software showing the time-course of the inlet temperature (upper panel, Temp. in °C) and gas flow (middle panel, Flow in mL.min<sup>-1</sup>) during the different PTV program steps (x scale in min).

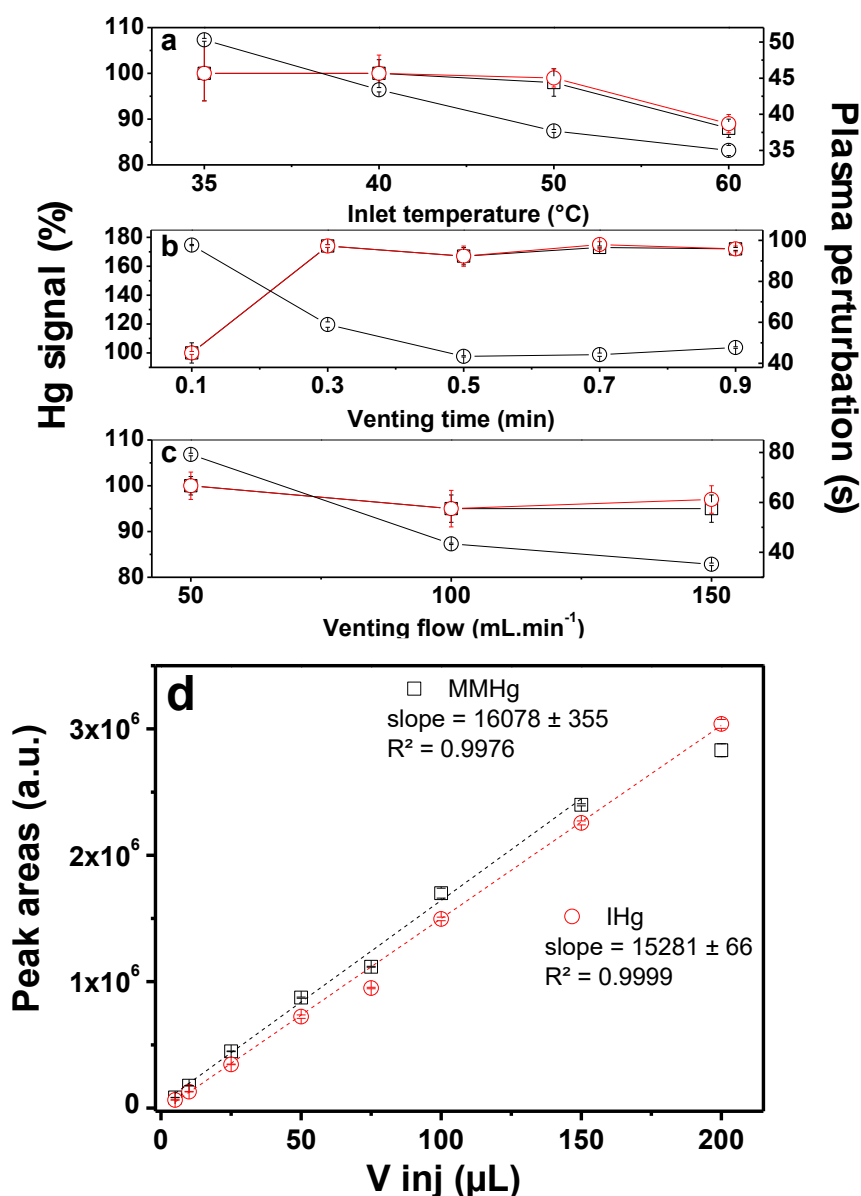


**Figure SI-3.** Upper panels: Normalized signal intensities of Hg species (MMHg black squares; IHg red circles) and duration of the plasma perturbation (black circles) as a function of (a) the inlet temperature (venting time and flow set at 0.5 min and 100 mL.min<sup>-1</sup>, respectively); (b) the venting time (Inlet temperature and venting flow set at 40 °C and 100 mL.min<sup>-1</sup>, respectively) and (c) the venting flow (Inlet temperature and venting time set at 40 °C and 0.5 min, respectively). The signal intensities of Hg species were first normalized to the TI signal to account for the instrument drift in sensitivity and then to the first conditions for each panel. Lower panel: Peak areas for each Hg species (50 pg.mL<sup>-1</sup>) as a function of the injected volume (single or 'at-once' injection until 75 μL, then multiple injections of 50 μL to reach the desired volume; points 75 and 200 μL discarded from the regression line for MMHg, 75 μL discarded from the regression line for IHg).

*Performances and validation with environmental reference materials.* Figure SI-3d presents the Hg species peak areas as a function of the injected volume. For single injections, they increase linearly up to 50 μL but at 75 μL both signals are approximately 10 % lower than expected. The maximum injectable volume 'at-once' is thus between 50 and 75 μL for each species but was not determine more precisely. For GC/MC-ICP-MS analysis, it is

indeed better to work below this maximum volume to avoid potential fractionation in the liner although this is not a problem for quantification by GC/Q-ICP-MS where such losses can be corrected. With multiple injections of 50  $\mu\text{L}$ , the maximum injectable volume could be extended to 150  $\mu\text{L}$  for MMHg and up to 200  $\mu\text{L}$  for IHg without losses. Over these ranges, the method linearity and reproducibility are very good ( $R^2 = 0.9976$  and  $0.9999$  for MMHg and IHg, respectively with  $\text{RSD} < 1.9\%$ ,  $n = 3$ ). Examples of calibration curves achieved are given in Figure SI-4 for two different volumes. The absolute DLs achievable with GC/Q-ICP-MS are down to  $0.2$  and  $0.8\text{ pg.L}^{-1}$  for IHg and MMHg respectively for an injected volume of  $200\text{ }\mu\text{L}$ . The methodological DLs are  $2$  and  $24\text{ pg.L}^{-1}$  for MMHg and IHg respectively, and are currently limited by blank levels especially for IHg.

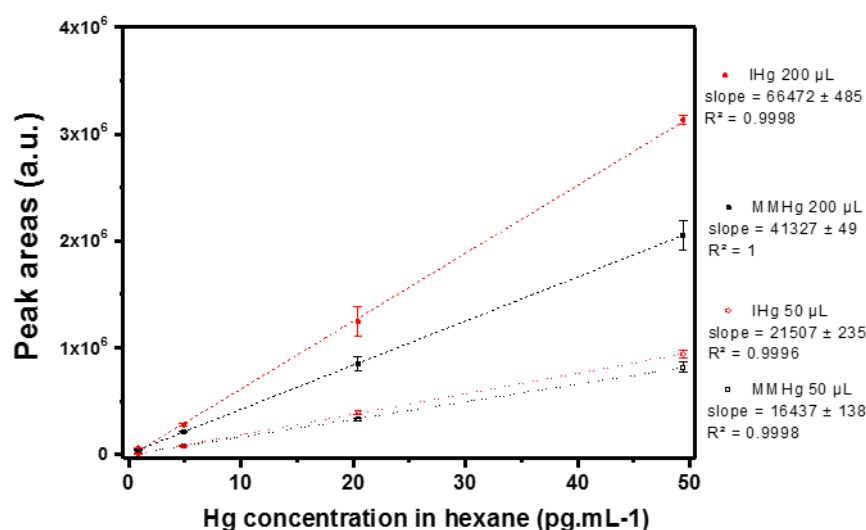


**Figure SI-4.** Calibration curves obtained for low level Hg species concentrations and two volume of injection ( $50$  and  $200\text{ }\mu\text{L}$ ).

The robustness of the technique to various real matrices was evaluated by the analysis of various environmental RMs (sediments, plankton, fish or crustacean tissues and organs), exhibiting HgT concentrations ranging from  $276$  to  $5240\text{ }\mu\text{g.kg}^{-1}$  and % MMHg/HgT from  $0.2$  to  $98\%$ . Hg species concentrations measured by conventional and PTV-GC/ICP-MS are presented in Table SI-1. Both techniques gave the same results (paired sample t test,  $p > 0.01$ ) demonstrating the suitability of the former for the analysis of environmental samples. Recoveries are overall satisfactory, usually between  $90$  and  $100\%$ , with the exception of the DOLT-4 and BCR-414 for which they are around  $80\%$ . Basic extractants may perform better than acidic ones for such samples but only the most common acidic extraction was tested in this work.

**Table SI-1.** Hg species concentrations measured in the various environmental RMs by regular GC/Q-ICP-MS and PTV-GC/Q-ICP-MS.

SRM	Material		Certified values (av ± sd)	n <sup>a</sup>	Regular GC/Q-ICP-MS		PTV-GC/Q-ICP-MS	
					(av ± sd)	Recovery <sup>b</sup>	(av ± sd)	Recovery
ERM CE-464	Tuna fish muscle	HgT	5240 ± 100	9	5009 ± 319	96 ± 6	ND	
		MMHg	5117 ± 170		4886 ± 316	95 ± 6		
NIST SRM-1947	Trout tissue	HgT	941 ± 19	9	907 ± 20	96 ± 2	908 ± 27	97 ± 3
		MMHg	863 ± 37		861 ± 29	100 ± 3	857 ± 34	99 ± 4
NRC DOLT-4	Dogfish liver	HgT	2580 ± 220	9	2193 ± 80	85 ± 3	2149 ± 93	83 ± 4
		MMHg	1330 ± 120		1052 ± 4	79 ± 0.3	1052 ± 9	79 ± 1
NRC TORT-2	Lobster hepatopancreas	HgT	270 ± 60	9	263 ± 6	97 ± 2	274 ± 12	101 ± 4
		MMHg	152 ± 13		138 ± 2	91 ± 1	138 ± 1	91 ± 1
NIST SRM-1944	Contaminated marine sediment	HgT	3400 ± 500	9	3576 ± 202	105 ± 6	ND	
		MMHg			7 ± 4			
IAEA-405	Estuarine sediments	HgT	810 ± 40	9	819 ± 59	101 ± 7	763 ± 54	94 ± 7
		MMHg	5.5 ± 0.5		5.4 ± 0.3	99 ± 5	5.8 ± 0.1	105 ± 2
ERM BCR-414	(Zoo)plankton	HgT	276 ± 18	9	227 ± 9	82 ± 3	225 ± 13	81 ± 5
		MMHg	208 ± 8		163 ± 2	78 ± 1	165 ± 4	79 ± 2

All concentrations expressed in  $\mu\text{g.kg}^{-1}$  dry weight; n = 9 ; recoveries are expressed as %

a. both RMs extractions and analyses in triplicate ; b. recoveries are expressed as %

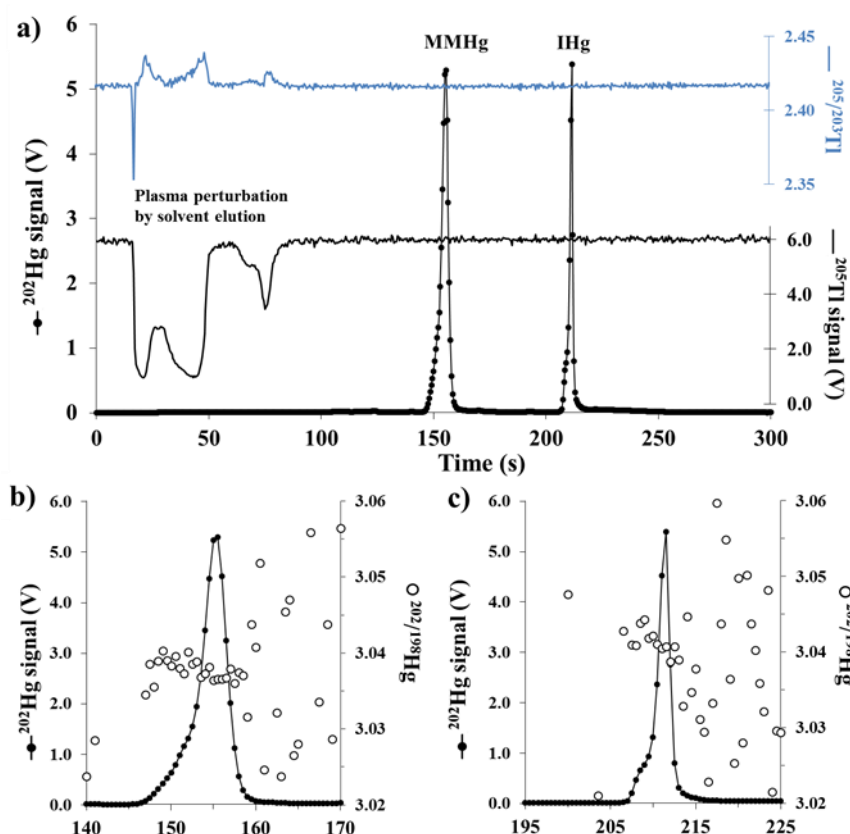


**Figure SI-5.** a) Typical example of a chromatogram displaying the Hg and Ti signals and isotopic ratios (Ti concentration = 200  $\mu\text{g.L}^{-1}$ ) for the analysis of a mix solution containing MMHg (STREM) and IHg (NIST-3133) standards (Injection volume is 25  $\mu\text{L}$  and Hg concentrations in hexane are 52  $\mu\text{g.L}^{-1}$  and 24  $\mu\text{g.L}^{-1}$ , respectively); b and c) zoom in MMHg and IHg signals and isotopic ratios (not corrected for mass bias) during species elution.

In the example given in Figure SI-5, the species-specific response is 1.7 times lower for MMHg compared to IHg when calculated based on peak heights (4.5 and 7.7  $\text{V}^{202}\text{Hg}.\text{ngHg}^{-1}$ , respectively) whereas it is similar when calculated based on peak areas (14.1 and 17.5  $\text{V}^{202}\text{Hg}.\text{s.ngHg}^{-1}$ , respectively). Over a selected subset ( $n = 132$ ) of all the STREM MMHg and NIST SRM-3133 IHg standards analyzed ( $n = 565$ ), the species-specific response varied within a factor less than 2 for MMHg (range 12 – 20  $\text{V}^{202}\text{Hg}.\text{s.ngHg}^{-1}$ , average  $14 \pm 2$ ) but 4 for IHg (range 5 – 20  $\text{V}^{202}\text{Hg}.\text{s.ngHg}^{-1}$ , average  $9 \pm 4$ ). These variations originate from a drift in the instrument sensitivity (regular fluctuations and instrument optimization between the various sequences) but also from the retention capacity of the packing material that slightly decreases over time. These sensitivities are similar to previous GC/MC-ICP-MS measurements but lower than the CVG-DGA introduction system (30 - 36  $\text{V}^{202}\text{Hg}.\text{s.ngHg}^{-1}$ ) for which the dry plasma conditions likely promote a more efficient Hg ionization.



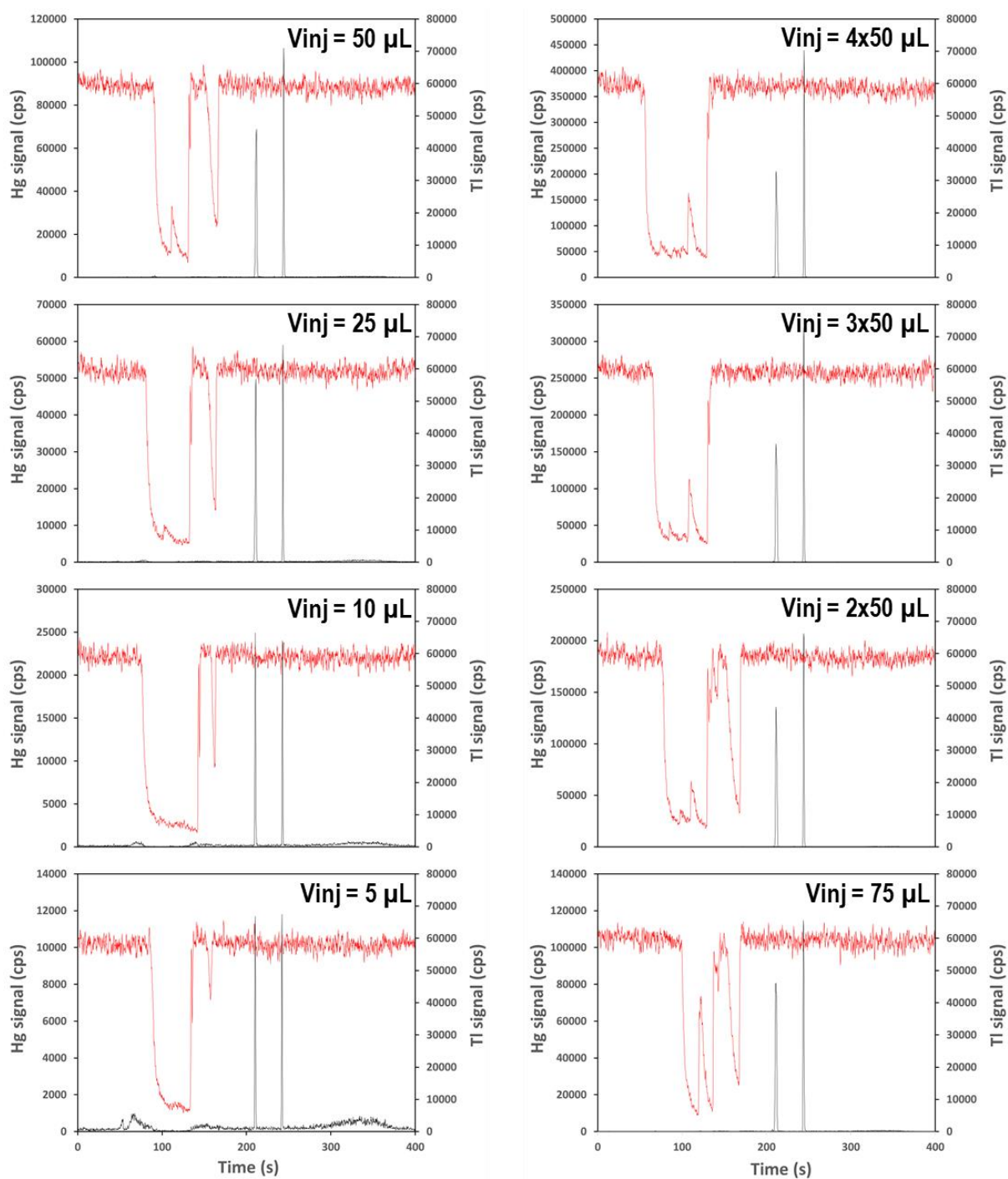


**Figure SI-6.** Typical examples of GC/Q-ICP-MS chromatograms obtained for the various injection volumes.

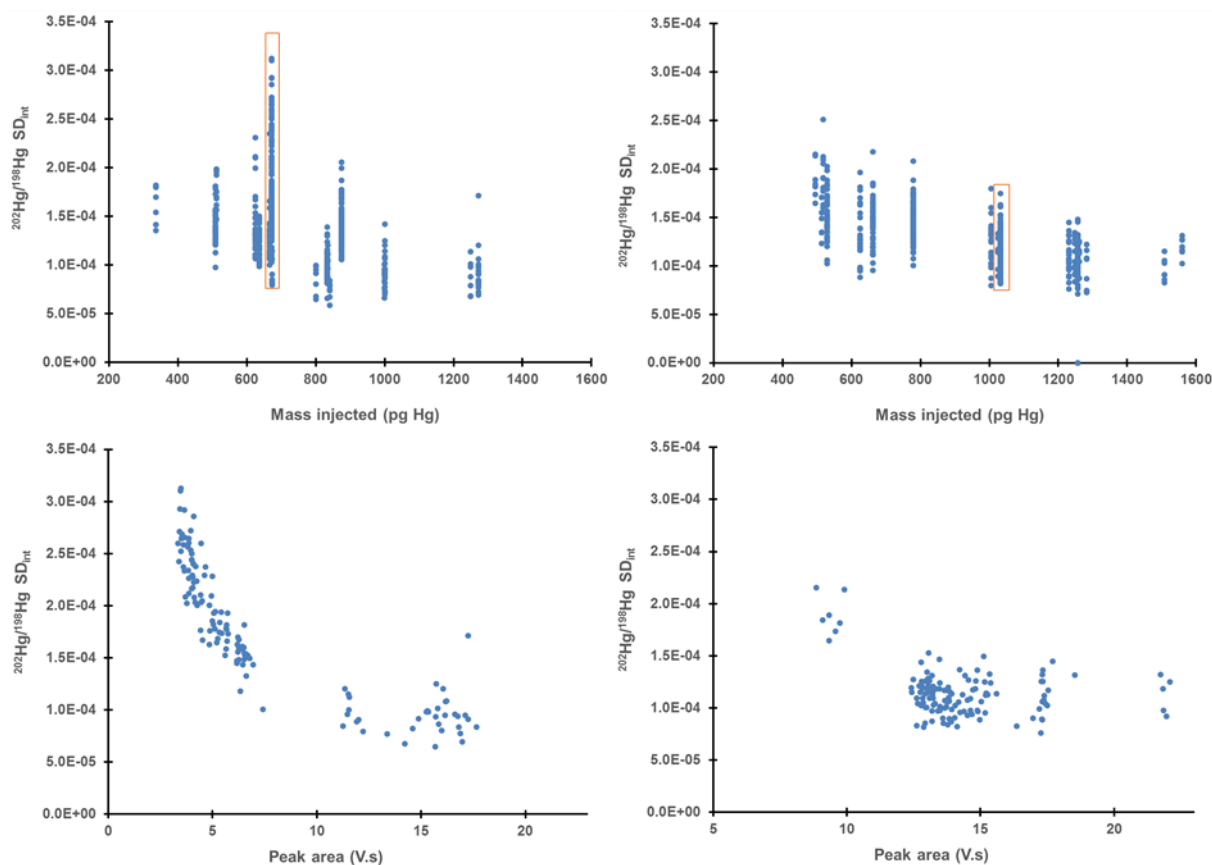


**Figure SI-7.** Internal precision on the  $^{202}/^{198}\text{Hg}$  isotopic ratio measurements for the NIST SRM-3133 IHg standard (left) and STREM MMHg standard (right) as a function of the Hg mass injected (upper panels,  $n = 565$ ) and peak areas (lower panels,  $n = 132$ ). Red boxes indicate specific sessions where samples containing high DOM content were analyzed suggesting a larger impact on the internal precision of IHg than MMHg.

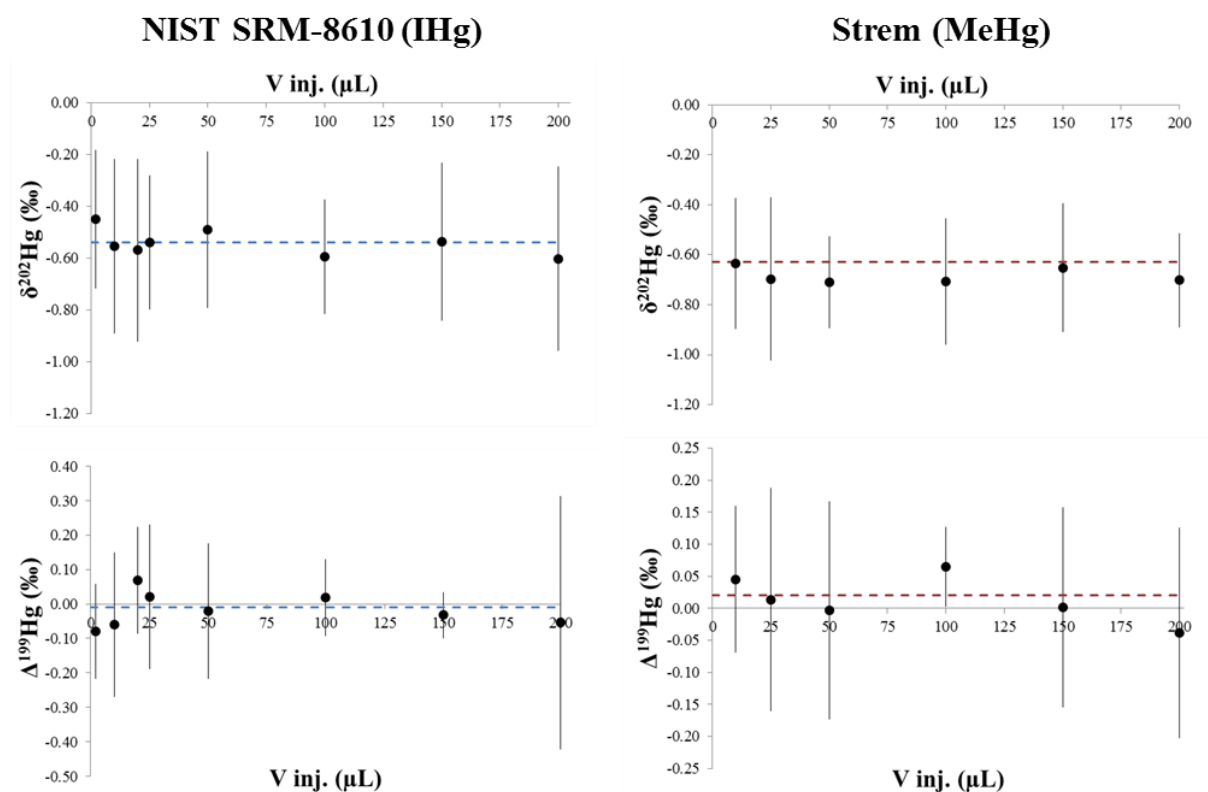


**Figure SI-8.** Isotopic compositions of IHg NIST SRM-8610 and MMHg STREM standards versus NIST SRM-3133 as a function of the injected volume. Each point is the average of 6-25 measurements and error bars represents 2SD. For the MMHg STREM standard, deltas values are calculated using the CSB procedure. Dashed lines represent previously published values determined with CCVG/MC-ICP-MS (IHg NIST SRM-8610 (Blum and Bergquist 2007):  $\delta^{202}\text{Hg} = -0.56 \pm 0.03$  and  $\Delta^{199}\text{Hg} = -0.03 \pm 0.02$  ‰ and MMHg STREM (Epov et al. 2010):  $\delta^{202}\text{Hg} = -0.63 \pm 0.15$  and  $\Delta^{199}\text{Hg} = 0.02 \pm 0.04$  ‰). Hg concentrations in the injected solution are given in Table SI-1.

**Table SI-2.** Injected volumes and the corresponding Hg concentrations in the organic solvent (hexane).

V inj (μL)	[Hg] in solvent (μg.L <sup>-1</sup> )
2	400-500
10	50-100
20	50
25	25-50
50	10-25
100	5-12.5
150	10
200	5

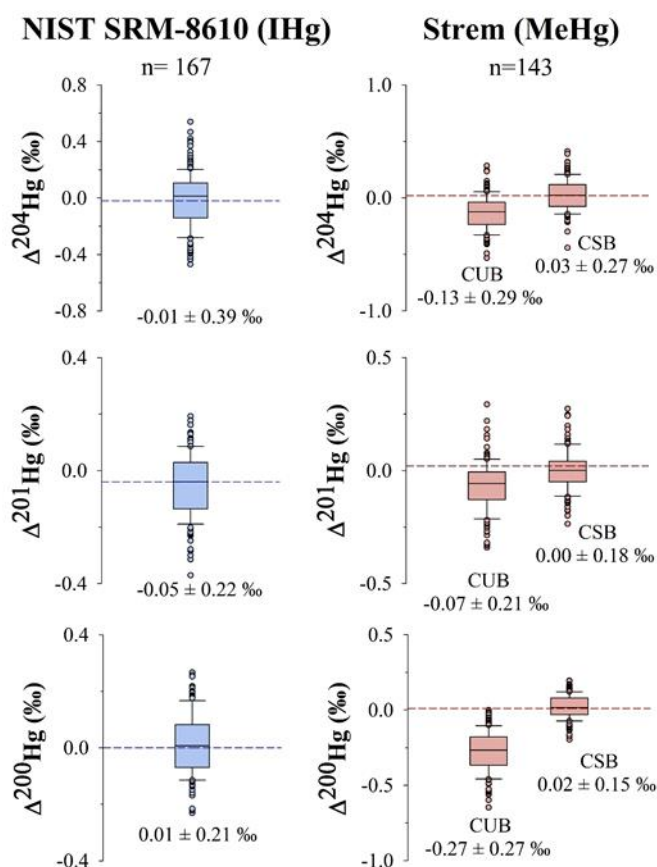


**Figure SI-9.** Distribution of the complementary MIF values (with respect to Figure 1) over 2 years of the NIST SRM-8610 and STREM standards (values given as average  $\pm$  2SD). For the MMHg STREM, results from both Compound Unspecific Bracketing (CUB) and Compound Specific Bracketing (CSB) calculation methods are presented. Dashed lines represent values determined with CCVG/MC-ICP-MS (Blum and Bergquist, 2007 for the NIST SRM-8610 and Epov et al., 2010 for the STREM standard).

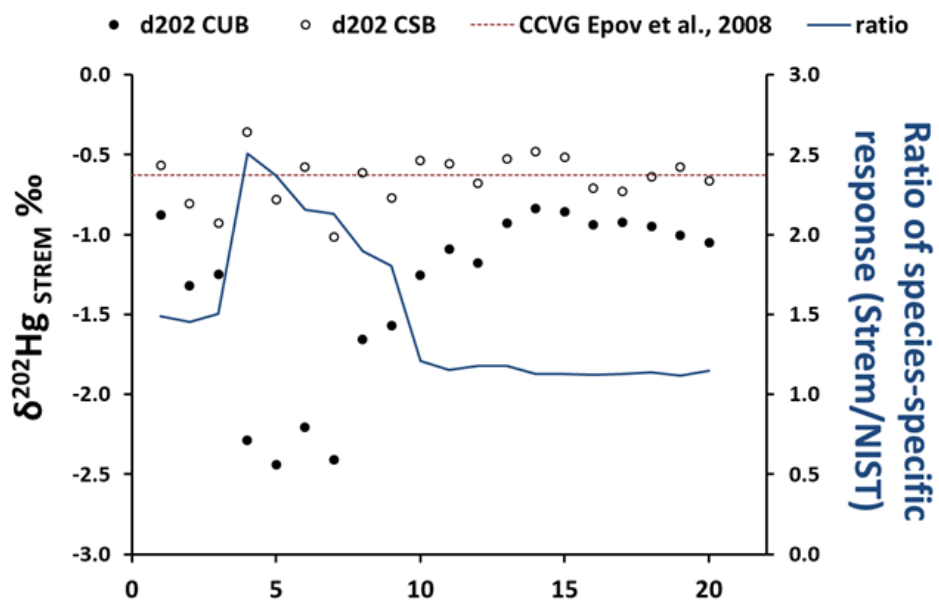


**Figure SI-10.** Example of  $\delta^{202}\text{Hg}$  STREM values calculated by CUB and CSB and confronted to the ratio of the species-specific response between the STREM and NIST 3133 standards.

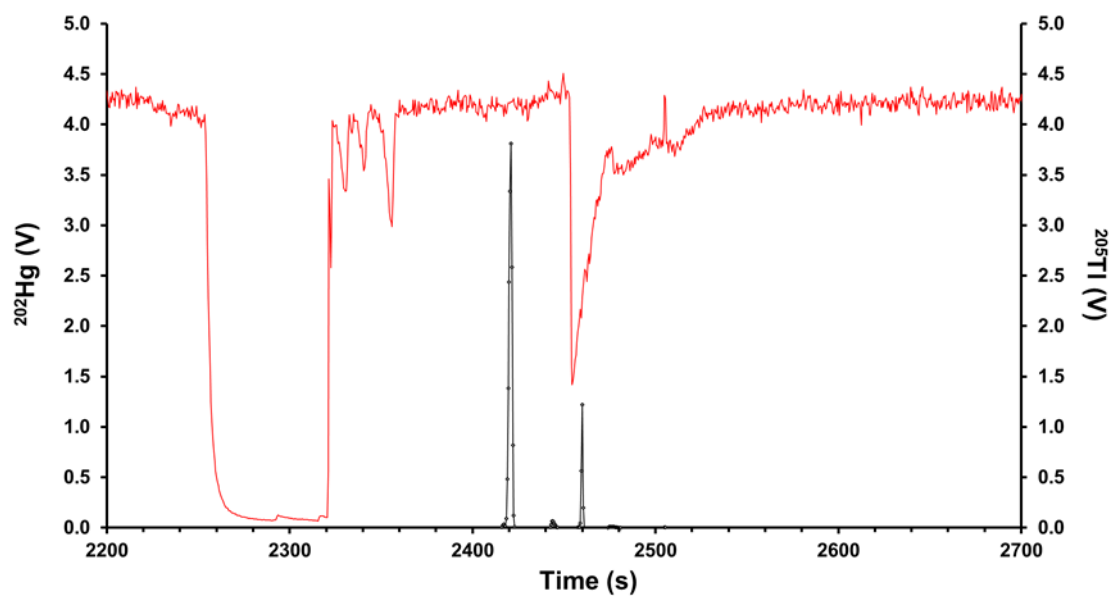


**Figure SI-11.** Typical chromatogram showing the TI perturbation during the IHg elution observed for the NRC TORT-2.